IMPROVEMENT OF ENERGY RESOLUTION OF ΔE-E CsI/SSD-TELESCOPE AT MEASUREMENT OF (γ,p)-REACTIONS USING STRIP INFORMATION OF SSD

G. Brudvik[1], D.D. Burdeinyi[2], V.B. Ganenko[2], K. Hansen[3], K. Fissum[3], L. Isaksson[3], K. Livingston[4], M. Lundin[1], B. Nilsson[1], B. Schröder[1,3]

[1]MAX-lab, Lund University, Lund, Sweden;

[2]National Science Center "Kharkov Institute of Physics and Technology", Kharkov, Ukraine;

[3]Department of Physics, Lund University, Lund, Sweden;

[4]Department of Physics and Astronomy, University of Glasgow, Glasgow, Scotland, UK

Information on the triggered strips of silicon strip detectors of a MAX-lab ΔE-E CsI/SSD-telescope was used to determination the angular range of emitted reaction particles. It allowed an improvement in the energy resolution of the telescope by decreasing the kinematical broadening of the missing energy spectra of $^{12}C(\gamma,p)^{11}B$ reaction, and enabling more accurate separation of exited states of residual nucleus.

PACS: 07.05.Kf, 24.70.+S

INTRODUCTION

In the energy range between the Giant Dipole Resonance and the pion photoproduction threshold (intermediate energy range) one-body and two-body effects may play an important role in photon interaction with nuclei. Of all possible photonuclear processes in this energy range, the (γ,N) reactions on light nuclei (^{12}C, ^{16}O), with separation ground and low lying exited states in the residual nucleus have most widely studied (see [1 - 5] and references within). One of the important results was the observation of a close similarity between the (γ,p) and (γ,n)-reaction cross sections [1, 4], strongly suggesting a two-body (quasi-deuteron (QD)) mechanism for photo-absorption by the nucleus, and suppression of the single nucleon direct knockout (DKO). One of the aims of the work presented here is the investigation of relative role of the DKO and OD mechanisms of a photon absorption. This requires precise experimental information on the cross section (and other experimental observables, as well) with indification of the final state of the residual nucleus.

One of the previous measurements of the carbon disintegration at MAX-lab [5] was in the 40…60 MeV energy range, using a tagged bremsstrahlung photon beam, thin carbon targets, and specially constructed proton telescopes, consisting of thin silicon and Ge detectors. The placement of the detectors in a vacuum box made it possible to achieve a resolution ≤ 1 MeV in the missing energy spectra, allowing the separation of the ground state of ^{11}B from the first exited state at E_{ex}=2.12 MeV. It also enabled the separation of the two maxima, at E_{ex} ~ 5 and ~ 7 MeV, resulted from unresolved states at E_{ex}= 4.44 and 5.02 MeV, and at E_{ex}=6.74, 6.79, 7.29 MeV, respectively.

Recent measurements of the cross section asymmetry, have also been made at MAX-lab, using a tagged linearly polarized photon beam [6, 7] and available

ΔE-E CsI/SSD-telescope. The telescope consisted of two silicon strip detectors (SSDs) and a CsI(Tl) counter, and was not optimized for high energy resolution at the $^{12}C(\gamma,p)^{11}B$ measurements. Hence it was not possible to resolve the ground and first exited states, and the peaks near 5 and 7 MeV. The poorer energy resolution was manly due to the fluctuation of ionization losses of the protons on their way from the target to the telescope, the intrinsic resolution of the CsI-detector, and kinematical broadening due to large angular capture An improvement in the energy resolution in this case can be achieved by decreasing the kinematical broadening, using coordinate information of the detected events from SSDs.

The telescope characteristics and method of the (γ,p)-reactions identification were described in [8] in detail.

1. EXPERIMENTAL APPARATUS AND DATA ANALYSIS

The measurements were made at the MAX-lab nuclear physics facility, described in detail in [9] and summarised hear. Electrons with energy E_0=192.7 MeV were extracted from the MAX-I ring, which operated a stretcher mode and delivered beam into experimental hall. A schematic of the MAX-lab beam line is shown in [7, 9]. Then electrons are directed towards photon bremsstrahlung radiators, 50 μm Al or 100 μm diamond, fixed in the target holder of a goniometer. A photon collimator with 12 mm opening was used for the photon beam formation on the target. The focal plane (FP) hodoscope of tagging system consisted of two rows of overlapping (50%) scintillators 25 mm wide and 3.2 mm thick. The coincidence requirement to overlapping scintillators resulted in 62 channels covering an energy range of E_γ=21.9…78.8 MeV. The resolution of the tagger system calculated for 50% overlap and normal incident of the scattered electrons to the MT focal plane was $\Delta E_\gamma \approx 0.8$ MeV for the high end of the tagged range, and smoothly increased to $\Delta E_\gamma \approx 1$ MeV at $E_\gamma \approx 38$ MeV.

The measurements were made on a CD_2 and CH_2 targets. The CD_2 target had a disc shape, of 75 mm in diameter, 1 mm thick, and density ρ=1.026 g/cm^3. The CH_2 target had square form, 150.2×150.2 mm and

1.1 mm thick, and the ρ=0.937 g/cm^3. The targets were positioned on distance of ≈ 2 m from the photon collimator at an angle of $\theta_m=60^0$ to the photon beam direction.

1.1. CsI/SSD-TELESCOPE

The emitted protons were detected by a CsI/SSD-telescope, schematically shown in Fig. 1. The telescope consists of two identical single-sided silicon strip detectors (SSDs) and a CsI(Tl)-counter. The SSD-detectors (ΔE) are of octagonal shape, have an active area of 3300 mm^2, and a thickness of 0.5 mm. They have 64 strips, each with a width of 1 mm. The strips are paralleled in groups of two for the read-out, thus yielding an effective strip width of 2 mm. The active aria of the detectors was wrapped Al foil 15 μk thick. The CsI(Tl)-detector (E) is a cylinder 12.5 cm in diameter and 10 cm long, placed in Al container. The thickness of the front wall of the container is 0.5 mm. The telescope was placed at angle of $\theta_p=90^0$ to the beam axis. The distance between the first SSD and center of the photon beam sport on the target was equal 98.5 mm, the distance between the SSDs was equal 15 mm, the distance between the second SSD and the CsI was equal 10 mm.

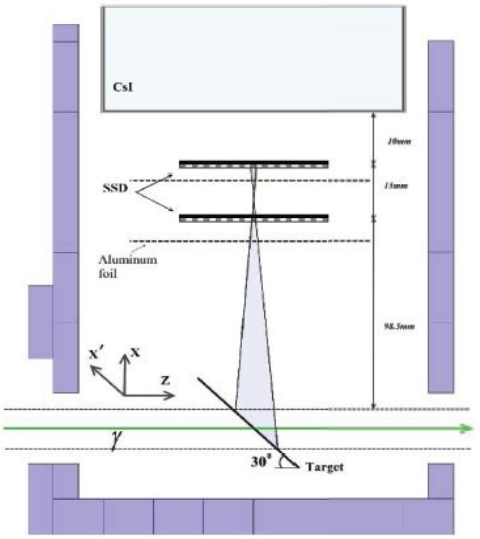

Fig. 1. Scheme of the SSD/CsI-telescope

1.2. DATA ANALYSIS

The data analysis was described in [8] in detail. It included three stages: proton identification, selection of prompt events, and reaction separation.

The proton identification were performed by standard ΔE-E method, based on relationship between the energy losses in a ΔE detector and full energy E of the particles with different masses. ADC signals from the SSDs (ΔE) and CsI (E) detectors were presented as two-dimensional $\Delta\tilde{E}$-E plot, in which the proton signals were separated from other particles signals (electrons, deuterons, etc.) into clear band. The background particles were removed by a soft cut on the plot.

The prompt events were obtained by selection of a time coincidence between the FP-detectors and the CsI/SSD-telescope signals. The coincidence searching technique was described in [8]. Having performed the procedure, the coincidence prompt peak appeared in the individual FPtdc spectra on top of random background. There are two types of events in the prompt peak region: true coincidence events from various channels of carbon and deuteron disintegration, an electromagnetic background, and random events. For separation yields of the d(γ,p)n and the $^{12}C(\gamma,p)^{11}B$ reactions, a missing energy (Emis) method was applied. It assumes of missing energy spectra construction of the reactions under study. The missing energy is given by relation,

$$E_m = E_\gamma - T_p - T_r,$$

where E_γ is the photon energy, T_p is the proton kinetic energy, measured by the CsI detector and corrected for energy losses of the proton on its way from the origin point to the detector. T_r is the energy of a recoil nucleus (neutron or ^{11}B), which is calculated using the reaction kinematics and the proton emission angle value $\theta_p=90^0$.

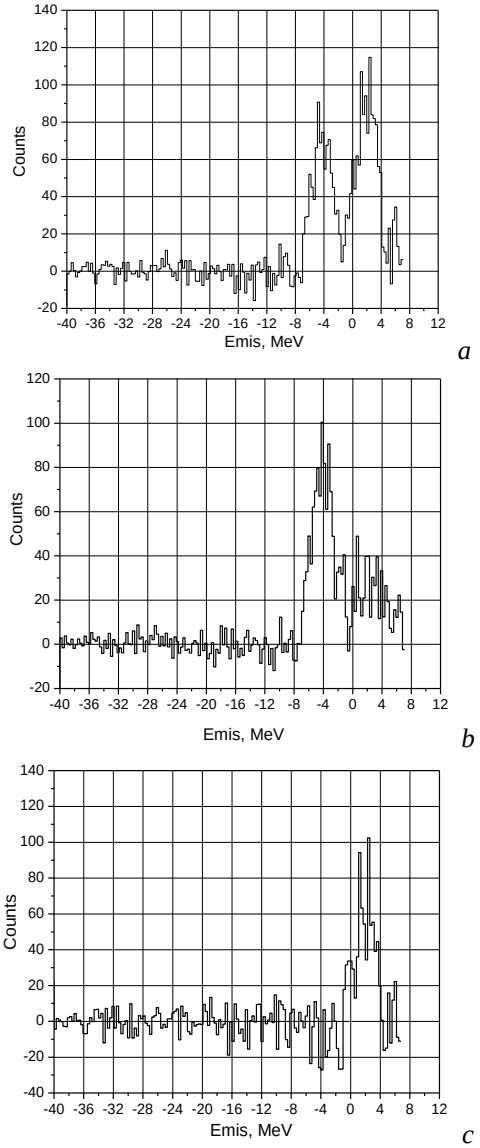

Fig. 2. Missing energy spectra of the protons from the CD_2 (a) and CH_2 (b) targets. (c) – the d(γ,p)n missing energy spectrum after the CD_2 and CH_2 spectra subtraction. Photon energy is E_γ=(49.0±2.0) MeV

After the random background subtraction (the procedure is descried in [8]) the final missing energy spectra are obtained. In order to increase statistics, summation of the

Emis spectra for four physically adjacent tagger channels was produced. As a result, the Emis spectra were obtained for eleven energy bins, with the width $\Delta E_\gamma \approx 4$ MeV. In Fig. 2 [8] the spectra for CD_2 and CH_2 targets at photon energy bin $E_\gamma = (49 \pm 2.0)$ MeV are shown. According to choice $T_r = T_n$, the events corresponding to reaction of the deuteron disintegration are located in a peak, whose position is equal to the deuteron binding energy, $E_{mis} \approx 2.2$ MeV (see Fig. 2,a). To the left side from this peak, there is a big maximum at $E_{mis} \approx -4$ MeV, corresponding to reaction of the carbon disintegration, $^{12}C(\gamma,p)^{11}B$, when the recoil nucleus ^{11}B is in the ground state or in the first exited state with excitation energy $E_{ex} = 2.12$ MeV. These states are not separated owing to insufficient energy resolution. There is also a weaker peak in the missing energy range $E_{mis} \approx 0 \ldots 4$ MeV (see Fig. 2,b), corresponding to the carbon disintegration, when the ^{11}B is in one of the excited states, $E_{ex} \sim 4.44$, 5.02, 6.74, 6.79 or 7.29 MeV, which are also not separated.

The energy resolution can be more accurate estimated from the spectrum of the d(γ,p)n-reaction, presented in Fig. 2,c. As can be seen, it is ~ 3.5 MeV (FWHM). As was stated the above, such energy resolution results from the telescope construction, in which too much matter was on the proton way (thick SSDs, targets, foils, air, etc.). That results in large ionization losses of the protons and their fluctuations, especially at small energies, and as a result, decreasing accuracy of the proton energy determination. Secondly, there is kinematical broadening of the peaks due to large angular acceptance of the telescope, in the case of standard procedure of the data taking, when only ΔE information is taken from the SSDs.

2. THE TELESCOPE ANGULAR ACCEPTANCE

The angular aperture of the CsI/SSD-telescope is determined by the sizes of the target active volume, the second SSD active aria, and the distance of the second SSD from the target. It was calculated by Monte Carlo simulation, using the GEANT-4 software package [10]. Three associated blocks of the experiment modeling were developed, described in [8] in detail. The first block includes simulation of the electron beam interaction with a photon radiator and passing of the bremsstahlung photon through the photon collimator on the target. As a result, the target active volume was determined. Its projection on the target plane, presented in [8], has an elliptic shape of ~14 mm (FWHM) in vertical, and ~ 28 mm in horizontal planes. The photon beam intensity distribution within this aria was obtained.

The second block simulated the passage of the protons produced in the target active volume from the reactions of the carbon and deuteron disintegration, tracing them through the telescope to the CsI. The proton energy losses were calculated, and the CsI detector energy calibration was produced.

The telescope angular acceptance was investigated in the third block. Using the accumulated data base, trajectories of the protons were constructed and their distributions over polar angle were calculated. Having the trajectories, the related SSDs strip numbers (the "triggered strips") were determined. It was found from the experimental data analysis [8] (and confirmed by the simulation results) that difference between the triggered strips of the first and the second SSDs, $\Delta = n_2 - n_1$, was within $|\Delta| \leq 3$ for all detected protons. n_1 and n_2 are the numbers of triggered strips in the first and the second silicon strip detectors, respectively, counted from the left to the right.

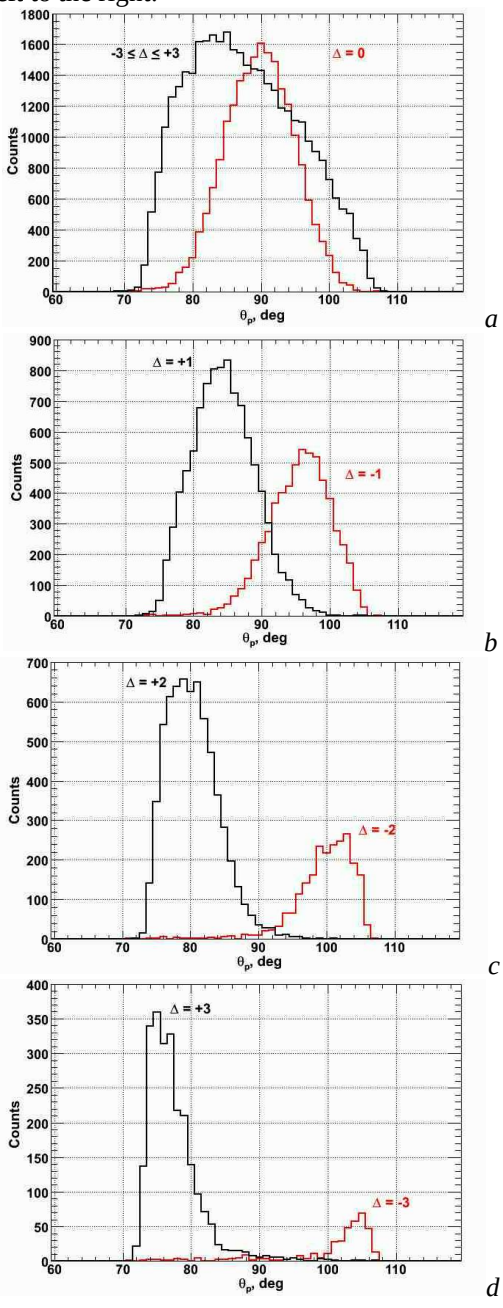

Fig. 3. Calculated angular capture of the SSD/CsI-telescope at the particle selection conditions: | Δ|≤3 and |Δ|=0 (a); Δ=±1 (b); Δ=±2 (c); Δ=±3(d)

The simulated trajectories of the protons were separated into seven groups determined under the triggered strips conditions: Δ=0, ±1, ±2, ±3, and the polar angle distributions of the proton emission for every group were calculated. Results of the simulation for the

$^{12}C(\gamma,p_0)^{11}B$-reaction, taking into account angular dependence of the corresponding cross sections from [5], are presented in Fig. 3. They show that in the case of detection of all particles, passing through the active aria of the SSDs ($|\Delta|\leq 3$), the telescope angular acceptance is $\Delta\theta_p \approx 30^0$ (FWHM). However, for the first group ($\Delta=0$), using events with identical triggered strip numbers in the first and the second SSDs, the angular capture is less, $\Delta\theta_p \approx 12^0$ (FWHM). In this case the detected particles are emitted from the whole active volume of the target, and pass predominantly within the central part of both SSD- detectors.

The trajectories selected into the next two groups ($\Delta = \pm 1$) correspond to the proton, emitted within angular intervals $\theta_p \approx (83\pm7)^0$ and $97^0\pm7^0$ (FWHM) for $\Delta=+1$ and $\Delta= -1$, respectively. The further two groups ($\Delta = \pm 2$) include trajectories of the protons, emitted within the angular intervals $\theta_p \approx 80^0\pm7^0$ and $\theta_p \approx 103^0\pm7^0$ (FWHM) for the $\Delta=+2$ and $\Delta = -2$ selection conditions, respectively, and from different parts of the target active aria. In the last groups ($\Delta=\pm 3$) there are trajectories corresponding to the protons, emitted within angular intervals $\theta_p \approx (73\ldots82)^0$ and $\theta_p \approx (100\ldots107)^0$ for selection conditions $\Delta=+3$ and $\Delta=-3$, from small part of the active target aria, being in opposite ends of the target.

For test of the simulation the calculated triggered strip number distributions in the first SSD were compared with the experiment data in the case of $^{12}C(\gamma,p)^{11}B$-reaction. The results of the simulation are in a reasonable agreement with the experiment. Fig. 4 shows distributions for two groups, $\Delta = 0$ and $\Delta = \pm 2$.

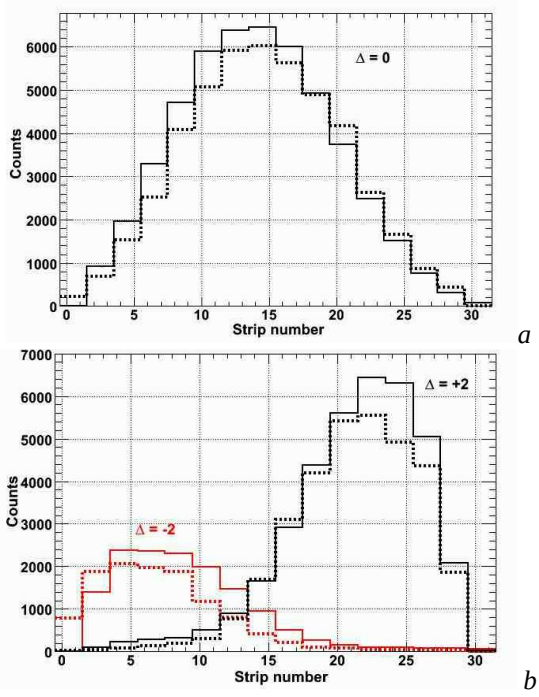

Fig. 4. Experimental (solid lines) and simulated (dotted lines) distributions of the triggered strip numbers in the first SSD for the particle selection conditions Δ=0 (a) and Δ=±2 (b). The distributions are summarized over odd and even strip numbers

Table 1

The effective angles of the proton emission, obtained from simulation $<\theta_p>_m$ and experiment $<\theta_p>_e$

Group (Δ)	-3	-2	-1	0
$<\theta_p>_m$,deg	101.2	100.2	96.0	89.8
$<\theta_p>_e$, deg		100.1±0.7	95.4±0.7	90.0±0.4
Group (Δ)	+1	+2	+3	–
$<\theta_p>_m$,deg	85.0	80.9	77.9	–
$<\theta_p>_e$, deg	83.8±0.6	80.7±0.4	–	–

The simulation demonstrates that the triggered strip information allows separation of the detected protons into seven groups with determination of an effective proton emission angle $<\theta_p>_m$ for each group, Table 1. For the reactions under study this separation results in different energies of the protons (the recoil nuclei, as well) for the selected groups at the given photon energies. So, Fig. 5 shows position of the ADC peak of the CsI signals resulted from the protons of the $\Delta=\pm 2$ and $\Delta=0$ (shown by solid line) groups, as a function of the photon energy. One can see that protons from these groups at the same photon energy produce different signals in the CsI, resulted from the difference of the proton energies. This difference should be taken into account at the Emis spectra construction.

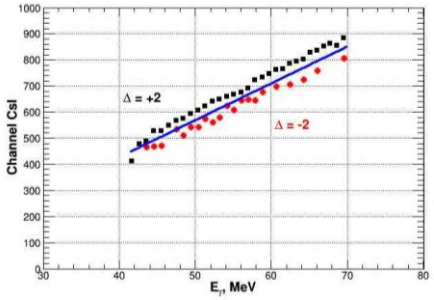

Fig. 5. ADC peak positions of the signals, detected by the CsI, from the protons of the Δ=±2 and Δ=0 (shown by solid line) groups for the $^{12}C(\gamma,p_0)^{11}B$-reaction, as a function of the photon energy

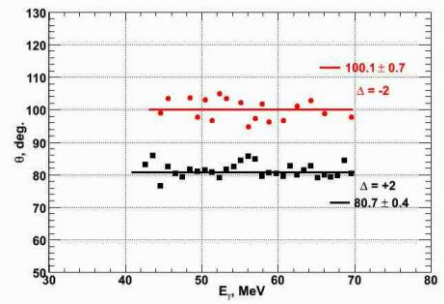

Fig. 6. Calculated effective angles of the proton emission for Δ=±2 groups, as a function of the photon energy

Using of the ADC peak positions and results of the CsI detector energy calibration [8], one can get the average energy of the detected protons from each group, and to calculate the proton emission angles from the kinematics. The angles were calculated by such a way for all groups (besides $\Delta=\pm 3$ due to poor statistics) as a function of the photon energy, as shown in Fig. 6. The angle's values for the given selected groups do not depend on the photon energy, fluctuating near effective values $<\theta_p>_e$, obtained by averaging the angles over

ISSN 1562-6016. ВАНТ. 2016. №3(103)

photon energy interval. The effective angles values, obtained by two methods well agree within the experimental errors and are presented in the Table 1.

Taking into account the effective proton emission angle values at the missing energy calculation, the missing energy spectra were obtained for the $^{12}C(\gamma,p_0)$- and the d(γ,p)-reactions for each from the seven groups, as a function of the photon energy, and positions of the peaks, corresponding to the d(γ,p) and $^{12}C(\gamma,p_0)^{11}B$-reactions were determined. Within the data accuracy, they coincide with the Q-values of the both reactions for all photon energies, ≈2.2 MeV for d(γ,p) and the ≈16 MeV for the $^{12}C(\gamma,p_0)^{11}B$-reactions, for all selected groups. The values averaged over photon energy interval are presented in the Table 2.

Table 2

Q-values of the $^{12}C(\gamma,p_0)$ and the d(γ,p) reactions for selected groups averaged over photon energy bins

Group (Δ)	-3	-2	-1	0
Q, MeV, $^{12}C(\gamma,p)$	15.92 ±0.38	15.89 ±0.41	15.94 ±0.32	15.97 ±0.06
Q, MeV, d(γ,p)	2.26 ±0.41	2.12 ±0.33	2.26 ±0.35	2.20 ±0.06
Group (Δ)	+1	+2	+3	–
Q, MeV, $^{12}C(\gamma,p)$	15.90 ±0.32	15.98 ±0.32	16.01 ±0.32	–
Q, MeV, d(γ,p)	2.09 ±0.32	2.27 ±0.32	2.29 ±0.45	–

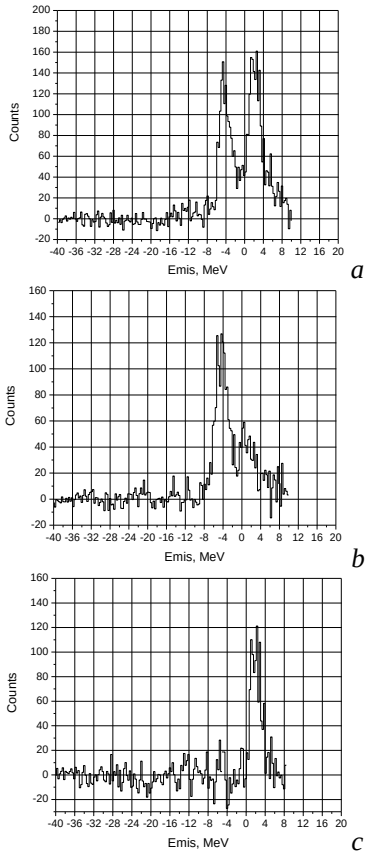

Fig. 7. The same missing energy spectra as in Fig. 2 after the kinematical broadening decreasing (see text)

The missing energy spectra taking into account information from SSDs triggered strips for calculation the energy of the recoil nucleus, are shown in Fig. 7, for the same experimental conditions, as in Fig. 2. The figures demonstrate more distinct peaks for both reactions, and the clear separation the ground and first exited states from the group of states at E_{ex}≈7 MeV. The energy resolution estimated from the peak of the d(γ,p)-reaction is ~2.2…2.5 MeV (FWHM). So, decreasing of the kinematical broadening allowed one to get more accurate missing energy spectra.

REFERENCES

1. P.D. Harty, M.N. Thompson, et al. $^{12}C(\gamma,n)$ cross section from 30 to 100 MeV // *Phys. Rev.* 1988, v. 37, p. 13.
2. S.V. Springham, D. Branford, T. Davidson, et al. A high-resolution study of the $^{12}C(\gamma,p)$-reaction with 49-78.5 MeV tagged photons // *Nuclear Physics*. 1990, v. A517, p. 93.
3. D.G. Ireland, D. Branford, T. Davinson, et al. The (γ,p)-reaction at E_γ~60 MeV // *Nuclear Physics*. 1993, v. A554, p. 173.
4. J.R.M. Annand, G.I. Crawford, P.D. Harty, et al. High resolution measurements of $^{12}C(\gamma,n)$ and the implications for the (γ,N)-reaction mechanism at intermediate energy // *Phys. Rev. Lett*. 1993, v. 71, p. 2703.
5. H. Ruijter, J-O. Adler, B-E. Andersson, et al. Angular distributions for the $^{12}C(\gamma,p)^{11}B$-reaction // *Phys. Rev.* 1996, v. C54, p. 3076.
6. V. Ganenko, K. Fissum, K. Hansen, et al. Production of linearly polarized photon beam at MAX-lab // *Problems of Atomic Science and Technology. Series "Nuclear Physics Investigations"*. 2009, № 3, p. 95-102.
7. V. Ganenko, J. Brudvik, D. Burdeinyi, et al. Linearly polarized photon beam at MAX-lab // *NIM*. 2014, v. A 763, p. 137.
8. D. Burdeinyi, J. Brudvik, V. Ganenko, et al. Measurement of (γ,p)-reactions with ΔE-E telescope at MAX-lab facility // *Problems of Atomic Science and Technology. Series "Nuclear Physics Investigations"*. 2015, № 3, p. 49-64.
9. J.-O. Adler et al. The upgraded photon tagging facility at MAX-lab // *NIM*. 2013, v. A715, p. 1-10.
10. http://geant4.cern.ch.

Article received 30.03.2016

УЛУЧШЕНИЕ ЭНЕРГЕТИЧЕСКОГО РАЗРЕШЕНИЯ ΔE-E CsI/SSD-ТЕЛЕСКОПА ПРИ ИЗМЕРЕНИИ (γ,p)-РЕАКЦИИ С ИСПОЛЬЗОВАНИЕМ ИНФОРМАЦИИ О СРАБОТАВШИХ СТРИПАХ МИКРОСТРИПОВЫХ ДЕТЕКТОРОВ

G. Brudvik, Д.Д. Бурдейный, В.Б. Ганенко, K. Hansen, K. Fissum, L. Isaksson, K. Livingston, M. Lundin, B. Nilsson, B. Schröder

Информация о сработавших стрипах кремниевых микростриповых детекторов была использована для более точного определения угловых интервалов детектируемых частиц ΔE-E телескопом CsI/SSD лаборатории Макс-лаб. Это позволило улучшить энергетическое разрешение телескопа путём уменьшения кинематического уширения спектров недостающей энергии реакции $^{12}C(\gamma,p)^{11}B$ и получить более точное разделение возбужденных состояний остаточного ядра.

ПОКРАЩЕННЯ ЕНЕРГЕТИЧНОЇ ЗДАТНОСТІ ΔE-E CsI/SSD-ТЕЛЕСКОПУ ПРИ ВИМІРЮВАННІ (γ,p)-РЕАКЦІЇ З ВИКОРИСТАННЯМ ІНФОРМАЦІЇ ПРО СПРАЦЬОВАНІ СТРІПИ МІКРОСТРІПОВИХ ДЕТЕКТОРІВ

G. Brudvik, Д.Д. Бурдейний, В.Б. Ганенко, K. Hansen, K. Fissum, L. Isaksson, K. Livingston, M. Lundin, B. Nilsson, B. Schröder

Інформація про спрацьовані стріпи кремнієвих мікростріпових детекторів була використана для більш точного визначення кутових інтервалів детектуючих частинок ΔE-E телескопом CsI/SSD лабораторії Макс-лаб. Це дозволило поліпшити енергетичну здатність телескопа шляхом зменшення кінематичного розширення спектрів недостатньої енергії реакції $^{12}C(\gamma,p)^{11}B$ і отримати більш точне розділення збуджених станів залишкового ядра.